I R A M P
8(2), December 2017, pp. 73-79

© International Science Press
ISSN: 2229-3159

Balmer-series hydrogen-beta line dip-shifts for electron density measurements

CHRSTIAN G. PARIGGER[1]*, CHRISTOPHER M. HELSTERN[1], KYLE A. DRAKE[1] AND GHANESHWAR GAUTAM[2]

[1] University of Tennessee, University of Tennessee Space Institute, Center for Laser Applications, 411 B.H. Goethert Parkway, Tullahoma, TN 37388-9700, USA
[2]Fort Peck Community College, 605 Indian Avenue, Poplar, MT 59255, USA
** Corresponding author E-mail: cparigge@tennessee.edu (C.G. Parigger)*

ABSTRACT: This research communicates electron density, N_e, measurements from recorded dip shifts of the 486.133 nm hydrogen beta line, H_β, of the Balmer series. Following laser-induced plasma generation in ultra-pure hydrogen gas at a pressure of 0.76×10^5 Pa (11 psi), the investigated N_e range is from 20×10^{17} cm^{-3} to 2×10^{17} cm^{-3} for time delays from optical breakdown of 25 ns to 275 ns, respectively. The experimental arrangement includes a 150 mJ, 6 ns Q-switched Nd:YAG laser device operated at the fundamental wavelength of 1064 nm. A 0.64 m spectrometer disperses and an attached gated detector records the emission from the plasma with a spectral system resolution of 0.1 nm. The results agree with standard full-width-at-half-maximum and peak-separation diagnostics, previously applied for N_e up to 8×10^{17} cm^{-3}. H_β dip-shift measurements indicate N_e of the order of 2 to 20×10^{17} cm^{-3}, also in accord with selected hydrogen alpha line, H_β, inferences from the line width. The electron temperature is of the order of 100,000 K, inferred from the ratio of line to 10-nm continuum and from a Boltzmann plot, 50 ns after initiation of optical breakdown.

PACS Codes: 52.70.-m, 32.30-r, 52.25.Jm, 42.62.Fi

Keywords: Plasma diagnostics, atomic spectra, plasma spectroscopy, laser spectroscopy, laser-induced breakdown spectroscopy.

1. INTRODUCTION

The hydrogen atom offers various plasma diagnostic opportunities in part due to interests in astrophysics redshifts in white dwarfs [1, 2], and in part due to extensive theory treatments and available spectroscopic information [1-6]. Applications include laser-induced breakdown spectroscopy [7] for characterization of the target composition. The Balmer series hydrogen alpha, hydrogen beta, and hydrogen gamma lines [8] are easily accessible in the visible, optical region of the electromagnetic spectrum. Full-width-at-half-maximum (FWHM) and peak-separation of the hydrogen beta line, H_β, yield an electron density, N_e, with reasonable, 5% accuracy [9]. However, bench-mark measurements show a linear relation in a log-log display of red shift versus N_e [10], investigated for red shifts up to 0.4 nm and N_e up to 5×10^{17} cm^{-3}.

In this work, the published results from a well-stabilized arc and electromagnetically-driven shocks are compared with laser-induced plasma generated using focused, Q-switched Nd:YAG radiation. The objectives include, first, to confirm the use of the published red-shift data [10], and second, to investigate the applicability of the linear log-log dependency for larger H_β red shifts up to 1 nm that are observed in optical breakdown micro-plasma.

2. POWER LAWS

For measurements of electron density, N_e, from the hydrogen beta line, H_β, empirical formulae are well tested in analysis of optical breakdown plasma emission spectroscopy [11]. The corresponding dip-shifts of H_β derived from

arc and electromagnetically-driven shock tube results [10], and presented in log-log graphical form, can be expressed as a power law for H_β dip-shift, $\Delta\delta_{ds}$,

$$\Delta\delta_{ds}[nm] = 0.14\left(\frac{N_e[cm^{-3}]}{10^{17}}\right)^{0.67\pm0.03} . \quad (1)$$

This relation, inferred from Figure 1 in Ref. [10], is established for dip shifts in between 0.03 to ~ 0.4 nm, and for N_e of 0.1 × 10^{17} cm^{-3} to ~ 5 × 10^{17} cm^{-3}. The FWHM, Δw_{H_β}, peak-separation, $\Delta\lambda_{ps}$, formulae from Ref. [11],

$$\Delta w_{H_\beta}[nm] = 4.5\left(\frac{N_e[cm^{-3}]}{10^{17}}\right)^{0.71\pm0.03} , \quad (2)$$

$$\Delta\lambda_{ps}[nm] = 1.3\left(\frac{N_e[cm^{-3}]}{10^{17}}\right)^{0.61\pm0.03} , \quad (3)$$

serve the purpose of determining the N_e for comparison with the H_β dip shift results.

3. EXPERIMENTAL DETAILS

The primary experimental components are typical for laser-induced breakdown spectroscopy and have been summarized previously, e.g., see Ref. [12], but are included for completeness. A Q-switched Nd:YAG device (Quantel model Q-smart 850) is operated at the fundamental wavelength of 1064-nm to produce full-width-at-half-maximum 6-ns laser radiation with an energy of 850 mJ per pulse attenuated to 150 mJ per pulse. A laboratory type Czerny-Turner spectrometer (Jobin Yvon model HR 640) with a 0.64-m focal length is equipped with a 1200 grooves/mm grating and an intensified charge coupled device (Andor Technology model iStar DH334T-25U-03) for recording of temporally and spatially resolved spectral data. The equipment includes a laboratory chamber or cell with inlet and outlet ports together with a vacuum system, electronic components for synchronization, and various optical elements for beam shaping, steering and focusing.

4. RESULTS AND DISCUSSION

The experimental series for the measurement of H_β included first evacuating the cell using a mercury pump, and then filling the cell to a pressure of 0.76 × 10^5 Pa (11 psi) with ultra-high pure hydrogen gas. Just like in recently reported CN measurements [12], optical breakdown was generated inside the chamber at a rate of 10 Hz, with the laser beam focused with f/5 optics from the top, or parallel to the slit. The detector pixels are binned in 4 tracks along the slit direction to collect 256 spectra for each time delay. In an individual experimental run, data from 100 laser-plasma events are accumulated for 13 time delays in steps of 25 ns, and using a gate-open duration of 5 ns. Wavelength and sensitivity calibrations for each of the 256 background-contribution subtracted, recorded spectra were accomplished with a standard hydrogen lamp and a deuterium and tungsten halogen light source (Ocean Optics model DH-2000-CAL), respectively.

Figure 1 displays time resolved plasma spectra, accumulated from 100 consecutive laser-induced sparks, in ultra high pure hydrogen gas below standard atmospheric pressure of 0.76 × 10^5 Pa (11 psi). The 1064 nm laser beam is focused from the top and parallel to the slit. The vertical axis indicates the slit dimension, the laser beam is focused using f/5 optics for the 150 mJ, 6 ns pulses. With 1:1 imaging in this work, the vertical plasma size in the cell amounts to ~ 5 mm. The spectra indicate the H_β double-peak structure and the dip-shift from the central 486.133 nm position. The images also provide an overview of the FWHM and continuum contributions.

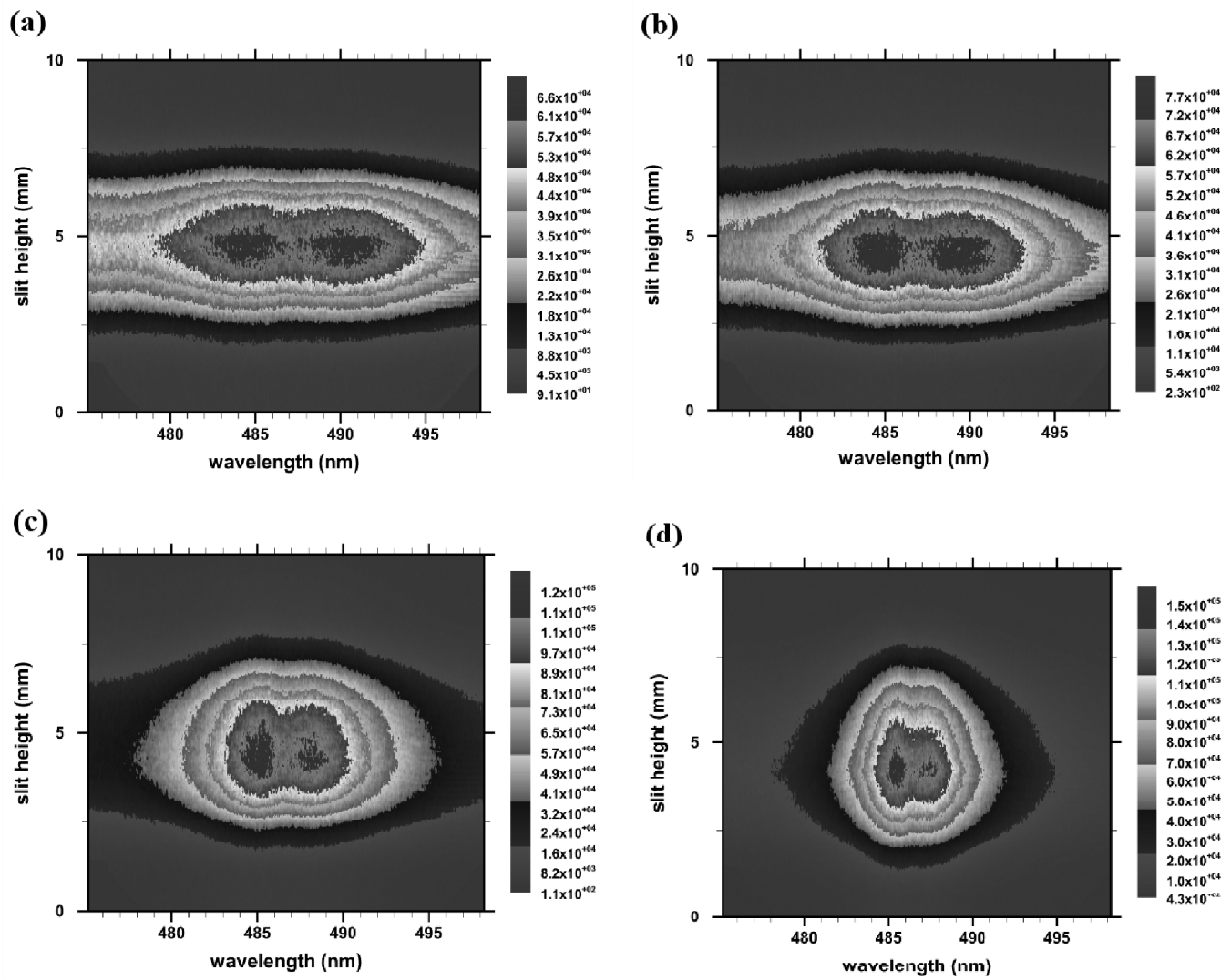

Figure 1: Measured H_β spectra. Gate width: 5 ns, time delay (a) 50 ns, (b) 75 ns, (c) 150 ns, and (d) 275 ns after optical brekadown in hydrogen gas at a pressure of 0.76×10^5 Pa (11 psi)

The two-dimensional pseudo-color representation of the central 184 of the 256 recorded spectra of Figure 1 indicate red shifts of the H_β dip that are larger earlier in the plasma evolution. The data of relative intensity versus wavelength would reveal dip-shift variations along the plasma for each time delay. Application of integral inversion techniques would also show the spatial variations similar to those reported recently [13]. Individual spectra contain ~ 10% peak-peak noise that would cause errors in determining dip-shifts, peak separations, and widths. The averages of 150 spectra, recorded from 100 consecutive laser-plasma events at a rate of 10 Hz, in the slit region of 1.6 mm to 9.7 mm yield average dip-shifts, peak separations, and widths. Fig. 2 shows these averaged line-of-sight data scaled by a factor of 100 but otherwise corresponding to the images of Fig. 1 (a) to (d), respectively.

The values for the dip-shift and peak separation show relatively large error bars due to the shallow dips and peaks, and in part due to the averaging of measured spectra along the slit. It is also difficult to determine the full-width at half maximum due to the significant free electron background contributions, and for Stark broadening with FWHM that appears larger than the spectral window for shorter time delays. Table 1, indicates the data and computed N_e for different time delays in the range of 25 ns to 275 ns. Instead of fitting available, full H_β profiles to determine FWHM and peak separations, as communicated earlier for evaluation of radial profiles [14], the spectrum yields the

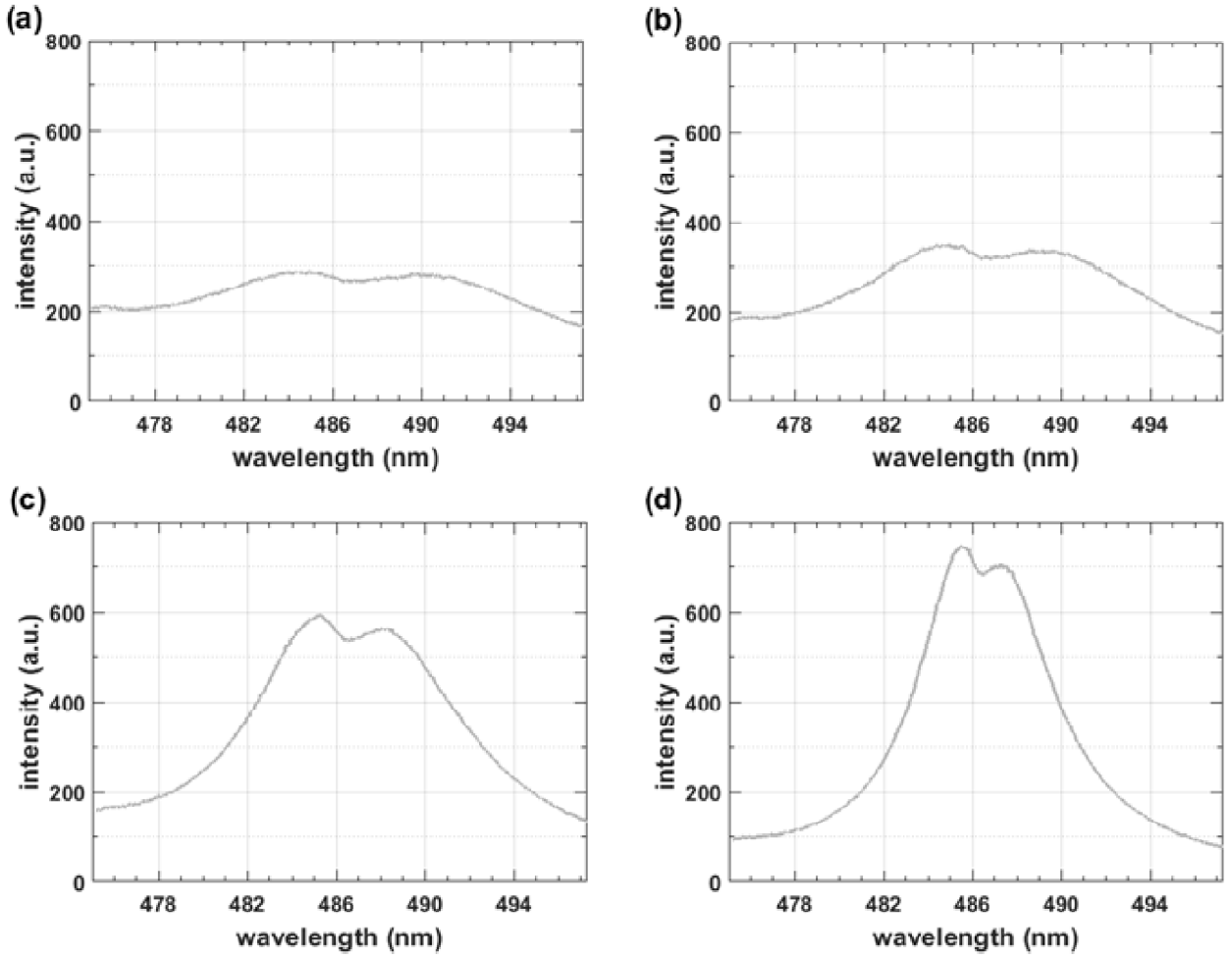

Figure 2: Average spectra of H_β. Gate width: 5 ns, time delay (a) 50 ns, (b) 75 ns, (c) 150 ns, and (d) 275 ns, for a hydrogen gas pressure of 0.76×10^5 Pa (11 psi)

three parameters for dip-shift, ds, peak-separation, ps, and FWHM, w. At the time delay of 25 ns, the H_β dip-shift of 1.02 nm in Tab. 1 implies an electron density of 20×10^{17} cm^{-3}, and with N_e in the range of $15 - 24 \times 10^{17}$ cm^{-3}.

Table 1
Average H_β dip-shift, ds, peak separation, ps, full-width at half-maximum, w, for time delays, τ, of 25 ns to 275 ns after optical breakdown, and electron density values inferred from Equations (1) to (3)

τ (ns)	ds (nm)	ps (nm)	w (nm)	N_{ds} (10^{17}cm^{-3})	N_{ps} (10^{17}cm^{-3})	N_w (10^{17}cm^{-3})
25	1.02 ± 0.15	7.5 ± 0.9	–	15 – 24	14 – 21	– (H_α: 17)
50	0.83 ± 0.15	5.3 ± 0.8	–	11 – 19	7.6 – 13	– (H_α: 14)
75	0.77 ± 0.1	4.6 ± 0.8	~ 25	10 – 15	5.8 – 10	~ 11 (H_α: 11)
100	0.65 ± 0.1	4.4 ± 0.6	~ 23 ± 4	7.7 – 12	5.8 – 9.1	~ 10
125	0.58 ± 0.1	3.8 ± 0.5	~ 21 ± 4	6.3 – 11	4.6 – 7.1	~ 8.8
150	0.50 ± 0.1	3.2 ± 0.4	~ 15 ± 3	4.8 – 8.9	3.5 – 5.3	~ 5.5 (H_α: 5.6)
175	0.42 ± 0.1	2.8 ± 0.3	11 ± 2	3.5 – 7.2	2.9 – 4.2	3.5
200	0.37 ± 0.1	2.4 ± 0.3	9 ± 1	2.7 – 6.1	2.2 – 3.3	2.7
225	0.32 ± 0.1	2.3 ± 0.2	8 ± 0.5	2.0 – 5.2	2.2 – 2.9	2.3
250	0.26 ± 0.05	2.0 ± 0.2	7.5 ± 0.5	1.8 – 3.3	1.7 – 2.4	2.1
275	0.24 ± 0.05	1.9 ± 0.2	7.0 ± 0.5	1.6 – 3.0	1.6 – 2.2	1.9 (H_α: 1.9)

Table 1 also includes selected values from hydrogen alpha line, H_α, measurements of the line widths for the same experimental conditions, but for separate runs for H_α data collection. For the 25 ns and 50 ns time delays, H_β is too wide, but H_α confirms N_e obtained from the dip-shift of H_β when using the H_α formula for the line width from Ref. [11]. Figure 3 illustrates the H_β and H_α spectra measured at 25 ns time delay.

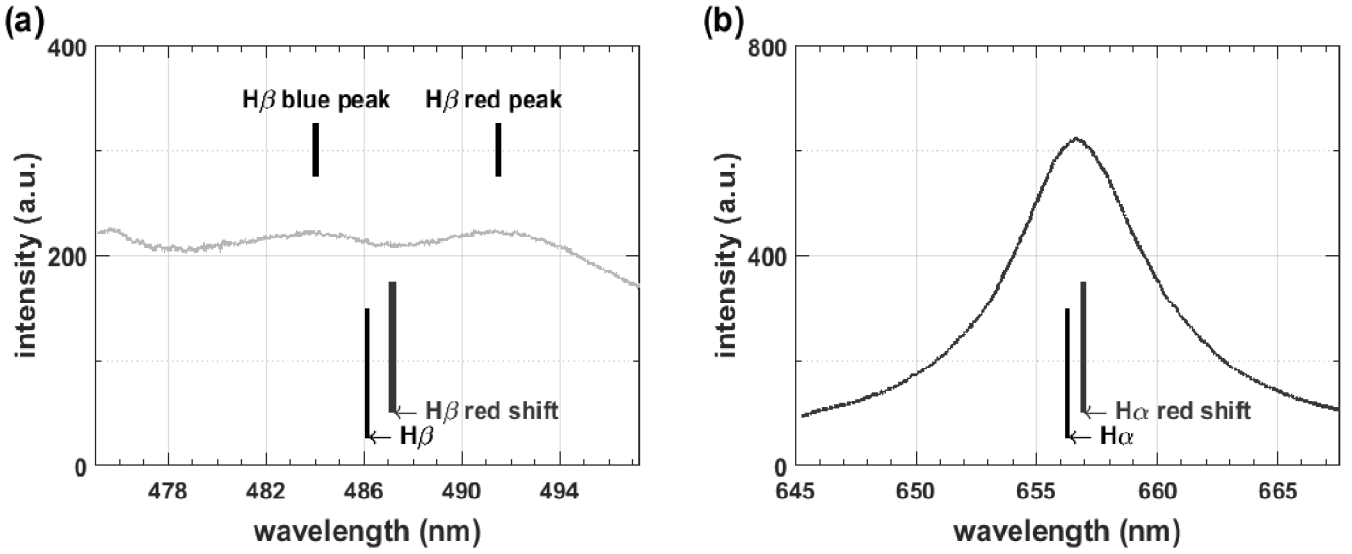

Figure 3: Average (a) H_β and (b) H_α line shapes. Gate width: 5 ns, time delay 25 ns. H_2 at 0.76 × 10^5 Pa (11 psi)

For the earliest time delays, the widths are larger than the spectral window, or larger than 25 nm. Values for N_e determined from peak separations and dip-shifts appear to agree within the error bars. The dip-shifts for the average spectra cause relatively large error ranges for N_e. Note, N_e can be reasonably determined from the FWHM of the H_β line but up to values of ~ 8 × 10^{17} cm^{-3} [15].

The electron temperature, T_e, determined from line to 10-nm continuum ratios [9, 16] and Boltzmann plots [17], ranges from 110 – 50 kK for time delays between 25 – 275 ns, respectively. For the earliest time delay of 25 ns (see Fig. 3) where there are indications of a slight dip and peaks, T_e is in excess of 100 kK (i.e., > 8.6 eV). Figure 4 displays the H_α spectra for time delays as in Fig. 2. Table 2 shows ratios of H_β and of 10-nm continuum, and T_e results obtained from data displayed in Fig. 13-6 in Ref. [9] or from recalculated ratios for T_e up to 140 kK.

Table 2
Ratio of H_β and of 10-nm continuum, and average electron temperature, T_e

τ (ns)	H_β ratio	T_e (kK)
25	1.9 ± 0.5	100 – 120 (H_α: 100 – 130)
50	2.3 ± 0.4	85 – 105 (H_α: 70 – 90)
75	3.0 ± 0.4	70 – 85 (H_α: 60 – 80)
150	3.5 ± 0.4	55 – 70 (H_α: 50 – 70)
275	4.2 ± 0.6	50 – 65 (H_α: 40 – 60)

Table 2 includes T_e values obtained from ratios of H_α and of 10-nm continuum [9, 16]. Although there are uncertainties in finding the 10-nm continuum contributions for both H_α and H_β, reasonable agreement is found for the electron temperature, T_e. Figure 5, displays the re-calculated [9] line to 10-nm continuum ratios versus temperature from 10 – 140 kK, and it also includes the data points and error estimates listed in Table 2.

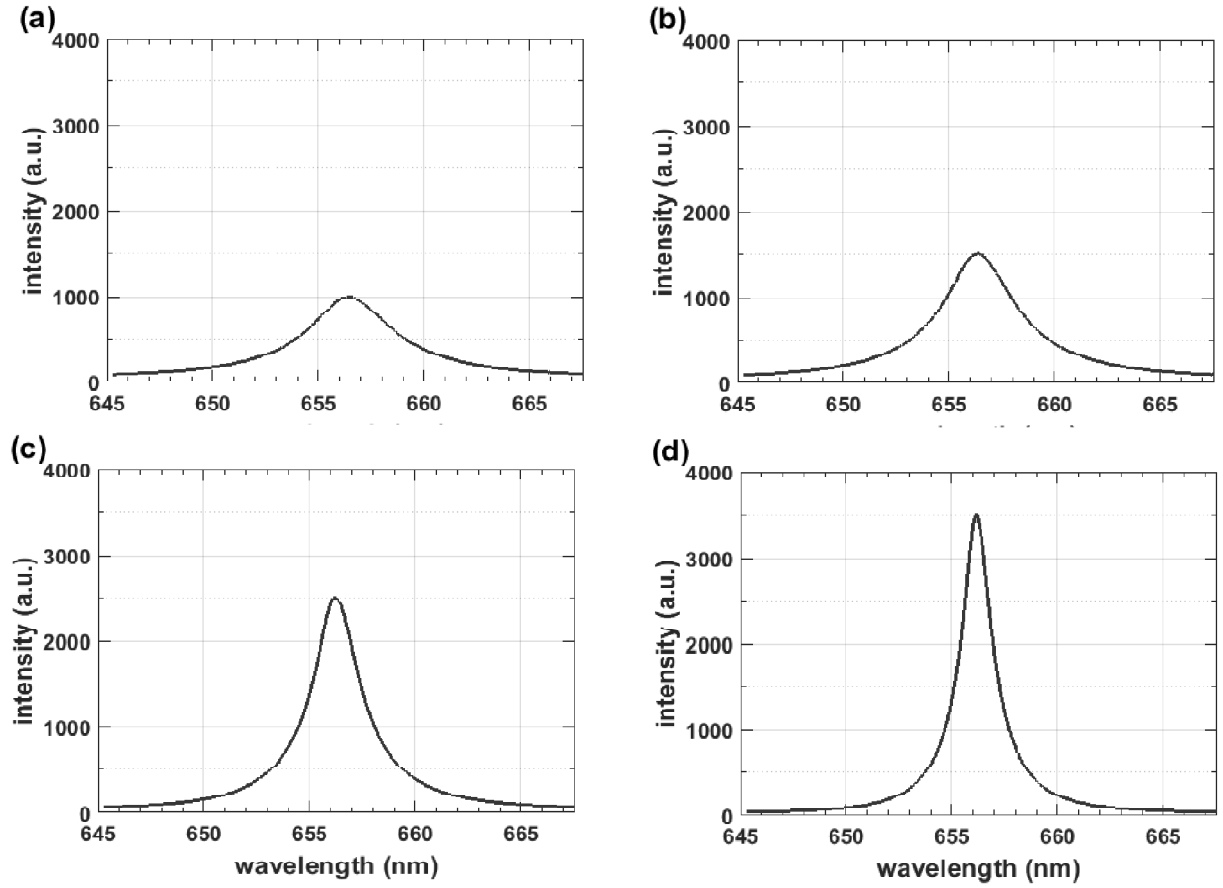

Figure 4: Average spectra of H_α. Gate width: 5 ns, time delay (a) 50 ns, (b) 75 ns, (c) 150 ns, and (d) 275 ns, for a hydrogen gas pressure of 0.76 × 10^5 Pa (11 psi)

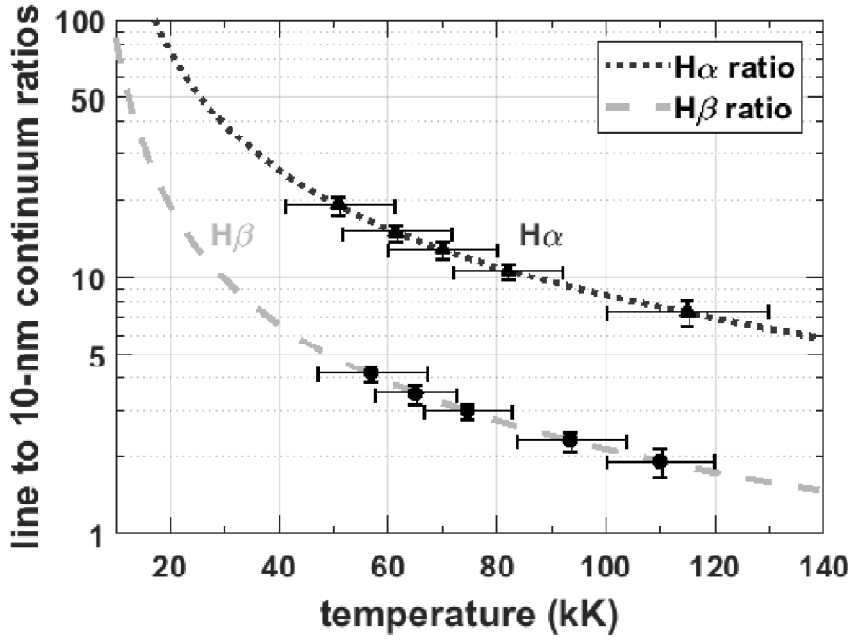

Figure 5: Computed H_α and H_β line to 10-nm continuum ratios. The date points from low to high temperature indicate results for 25 ns, 50 ns, 75 ns, 150ns, and 275 ns time delays from optical breakdown using 150 mJ, 6ns laser pulses at a wavelength of 1064 nm to generate micro-plasma in hydrogen gas at a pressure of 0.76 × 10^5 Pa (11 psi)

Results for T_e from standard Boltzmann plot analyses using H_α and H_β also agree with that of line to 10-nm continuum ratios. For example for a time delay of 150 ns, the integrated line ratio, H_β/H_α, amounts to 0.38 and is obtained from Figs. 2(c) and 4(c). A correction factor of 1.07 needs to be included because only 91% of H_α and 85% of H_β are recorded in the ~ 25 nm spectral window [17]. Consequently, from Figure 1 (a) in Ref. [17], or

$$T_e(eV) = 1/\ln[0.46/(H_\beta / H_\alpha)]^{1.5}, \quad (4)$$

the H_β/H_α ratio of 0.41 leads to a temperature of 67 kK (5.8 eV). The other results in Table 2 for T_e from line to continuum analysis agree as well with Boltzmann plot inferences. The computed H_β/H_α ratios [16, 17], or in other words Boltzmann plot methods, appear to be better suited for the 10 – 50 kK range as a flatter slope causes larger error margins in the 50 –100 kK range.

5. CONCLUSIONS

The analyses of Balmer series H_β line shapes reveal that the dip-shift of the central minimum delivers a third indicator of N_e. Comparisons with predictions from full-width at half maximum and from the H_β peak separation show agreement in the N_e range of $2 – 20 \times 10^{17}$ cm^{-3}. For lower densities, a resolution of 0.1 nm causes larger error bars, and for higher densities, larger error bars result due to broader line profiles. For N_e in excess of 8×10^{17} cm^{-3}, previously communicated as an upper limit for N_e determination from the Stark width of H_β, the dip-shift allows one to infer N_e up to ~ 20×10^{17} cm^{-3}. Moreover, the validity of the dip-shift diagnostics is extended from the previous shock tube studies of up to 5×10^{17} cm^{-3}, and the N_e results from H_β dip-shifts agree with that from H_α FWHM. Measured T_e are of the order of 100,000 K (8.6 eV) at a time delay of 50 ns from laser-induced breakdown. Of future interest are analysis of the spatial N_e and T_e distributions, including applications of Abel or Radon inversion techniques.

Acknowledgments

The authors thank for support in part by the Center for Laser Applications at the University of Tennessee Space Institute.

References

[1] J. Halenka, W. Olchawa, J. Madej, B. Grabowski, *Astrophys. J.* **808** (2015) 131.

[2] D. Koester, *Mem. S. A. It.* **81** (2010) 921.

[3] E. Oks, *Diagnostics of Laboratory and Astrophysical Plasmas Using Spectral Lineshapes of One-, Two-, and Three-Electron Systems*, World Scientific, Singapore, SG (2017).

[4] E. Oks, *Stark Broadening of Hydrogen and Hydrogenlike Spectral Lines in Plamas: The Physical Insight*, Alpha Science International, Oxford, GB (2006).

[5] S. Djurović, M. Ćirišan, A.V. Demura, G.V. Demchenko, D. Nikolić, M.A. Gigosos, and M.Á. González. *Phys. Rev. E* **79** (2009) 046402.

[6] C. Stehlé, M. Busquet, D. Gilles, A.V. Demura, *Laser Part. Beams* **23** (2005), 357.

[7] D.A. Cremers and L.J. Radziemski, *Handbook of Laser-Induced Breakdown Spectroscopy*, John Wiley and Sons, Hoboken, NJ, USA (2006).

[8] C.G. Parigger, A.C. Woods, J.O. Hornkohl, Appl. Opt. **51** (2012) B1.

[9] H.R. Griem, *Plasma Spectroscopy,* McGraw-Hill Book Company, New York, NY, USA (1964).

[10] J. Halenka, B. Vujićić, S. Djurović, *J. Quant. Spectrosc. Radiat. Transfer* **42** (1989) 571.

[11] D.M. Surmick, C.G. Parigger, *Int. Rev. At. Mol. Phys.* **5(2)** (2014) 73.

[12] C.G. Parigger, C.M. Helstern, G. Gautam, *Int. Rev. At. Mol. Phys.* **8(1)** (2017) 25.

[13] G. Gautam, C.G. Parigger, C.M. Helstern, K.A. Drake, *Appl. Opt.* **56** (2017) 9277.

[14] C.G. Parigger, G. Gautam, D.M. Surmick, *Int. Rev. At. Mol. Phys.* **6(1)** (2015) 43.

[15] C.G. Parigger, D.H. Plemmons, E. Oks, *Appl. Opt.* **42** (2003) 5992.

[16] S. Brieschenk, H. Kleine, S. O'Byrne, *J. Appl. Phys.* **113** (2013) 103101.

[17] G. Gautam, C.G. Parigger, *Int. Rev. At. Mol. Phys.* **6(2)** (2015) 83.